Understanding the Quantum Teleportation Protocol

Kurt T. Spranger[1], Michael R. Grimaila[1], and Douglas D. Hodson[2]
[1]Dept. of Systems Engineering and Mgmt., Air Force Institute of Technology, Wright-Patterson AFB, OH
[2]Dept. of Electrical & Computer Engineering, Air Force Institute of Technology, Wright-Patterson AFB, OH

Abstract – *Decomposing a complex system into smaller abstract functional blocks and developing mathematical models to represent their behavior is an important activity towards developing comprehensive system understanding. In this paper, we decompose the ideal Quantum Teleportation protocol into a collection of simple quantum circuit blocks, examine the behavior of each block, and show how collections of blocks operate to create more complex circuits. We believe this approach greatly simplifies the understanding of how the Quantum Teleportation protocol works. This paper is introductory in nature and is intended to help those who are new to modeling, simulating, and analyzing ideal quantum circuits.*

Keywords: Bell State Generation (BSG), Bell State Measurement (BSM), Einstein Podolsky Rosen (EPR) pairs, quantum entanglement, superdense coding, quantum teleportation.

1 Introduction

The evolution of quantum computing has driven the need for the development of quantum networks to interconnect geographically separated quantum computers [1,2]. The Quantum Teleportation protocol enables the transport of an arbitrary unknown quantum state from one location to another [3]. The goal of this paper is demonstrate how decomposing and abstracting the behavior of a complex system into a collection of smaller blocks can facilitate understanding of more complex behaviors. Specifically, we show how that decomposing the Quantum Teleportation protocol, an essential element of quantum networks, into its constituent blocks, studying the behavior of each block independently, and examining how interconnected collections of these blocks behave can simplify understanding of how the protocol works. The Quantum Teleportation protocol is often viewed as "magical" as it is the only way that one can transport an unknown quantum state from one location to another [2]. We seek to demystify this view to show that there is no "magic" behind the Quantum Teleportation protocol. One can easily understand how the protocol works by building a sound understanding of the mathematical abstractions of quantum mechanical blocks, examining the behavior of the constituent blocks, study the composition of collections of blocks, and by exercising simple mathematical analysis using college level algebra. In this paper, we assume the reader has a basic understanding of quantum information theory representations.

The remainder of the paper is organized as follows. Section 2 offers a basic introduction of the abstract mathematical modeling of two-level quantum mechanical system, Section 3 discusses the Bell State Generation (BSG) block used to generate maximally entangled Bell state pairs, Section 4 discusses the Bell State Measurement (BSM) block used to measure in the Bell basis, Section 5 considers the behavior of the BSG block connected to the BSM block, Section 6 presents the Superdense Coding protocol, and Section 7 presents Quantum Teleportation protocol. Finally, Section 8 concludes the paper and proposes our future work.

2 Mathematical Modeling of Two-Level Quantum Mechanical Systems

Quantum mechanics is a probabilistic theory in contrast to classical physics which is a deterministic theory [4]. While the classical bit is deterministically represented in one of two mutually exclusive values $\{0,1\}$, the *qubit* is a probabilistic representation in which the state of the qubit can be in a linear *superposition* of two possible orthogonal basis states: $\{|0\rangle, |1\rangle\}$. The state of a single qubit, $|\psi\rangle$, can be written as shown Eq. 1:

$$|\psi\rangle = \alpha|0\rangle + \beta|1\rangle \tag{1}$$

where α and β are complex numbers known as *probability amplitudes*, $|\alpha|^2 = (\alpha^*\alpha)$ is the probability of finding the qubit in the state $|0\rangle$, $|\beta|^2 = (\beta^*\beta)$ is the probability of finding the qubit in the state $|1\rangle$, subject to the normalization constraint $|\alpha|^2 + |\beta|^2 = 1$ [6]. A classical bit can be measured, copied, and reproduced without any loss of information. In contrast, a qubit generally cannot be measured without the likelihood of destroying information. The laws of quantum mechanics dictate that an unknown quantum state cannot be copied and resulted in the "No-Cloning Theorem" [5]. This is the exact reason why the Quantum Teleportation protocol is a required element to realize a quantum network: there is no other way to transport a generalized unknown quantum state from one location to another.

Note that the quantum state *Psi*, $|\psi\rangle$, is represented using Dirac's *ket* notation and equation (1) can be written as the $2x1$ column vector as shown in Eq. 2:

$$|\psi\rangle = \begin{bmatrix}\alpha\\ \beta\end{bmatrix} \tag{2}$$

The column vector contains the probability amplitudes in terms of the computational basis where the top element corresponds to the zero state, $|0\rangle$, and the bottom corresponds to the one state, $|1\rangle$ as shown in Eq. 3:

DOI 10.1109/CSCE60160.2023.00130

$$|0\rangle = \begin{bmatrix}1\\0\end{bmatrix} \text{ and } |1\rangle = \begin{bmatrix}0\\1\end{bmatrix} \quad (3)$$

The corresponding *bra* $\langle\psi|$ vector, denotes the conjugate transpose of $|\psi\rangle$ which is represented as $\langle\psi| = [\alpha^* \quad \beta^*]$. The inner product of two states $|\phi\rangle$ and $|\psi\rangle$, denoted as $\langle\phi|\psi\rangle$, is used to calculate the probability amplitude of measuring state $|\phi\rangle$ when in a known prepared state $|\psi\rangle$. This is a very important relation used frequently in quantum mechanics. When you take the inner product of two identical states, you obtain one (e.g., $\langle\psi|\psi\rangle = 1$). When the two states are orthogonal, you obtain zero (e.g., $\langle 0|1\rangle = 0$). The outer product of two states of two states $|\phi\rangle$ and $|\psi\rangle$, denoted as $|\phi\rangle\langle\psi|$, results in a matrix. For example, consider the outer product of $|0\rangle\langle 1|$ which can be calculated as shown in Eq. 4:

$$|0\rangle\langle 1| = \begin{bmatrix}1\\0\end{bmatrix}[0\ 1] = \begin{bmatrix}0 & 1\\0 & 0\end{bmatrix} \quad (4)$$

2.1 Quantum Logic Gates

Quantum logic gates are fundamental building blocks in quantum computation and are used to transform quantum states. In the sections that follow, we present the quantum gates that are found in the ideal Quantum Teleportation protocol. Quantum logic gates can be thought of as operators represented by unitary matrices acting on a two-level system. In this discussion, all transformations are with respect to the computational basis $\{|0\rangle, |1\rangle\}$ and are unitary. Any linear transformation on a complex vector space can be described by a matrix operation. Consider $A^\dagger$, the conjugate transpose of A. A is unitary if and only if $AA^\dagger = 1$. Unitary transforms can be thought of as rotations of complex vector space. Ideal quantum gates are reversible. If you apply the same operator to a quantum state twice in a row, the you obtain the original state you started with.

Before applying a unitary matrix to a multiple qubit state, you must first take the tensor product of the qubits to create a joint state. For example, if you have two qubits $|\phi\rangle$ and $|\psi\rangle$ that are input to a two-qubit quantum gate, you must first generate the joint state $|\upsilon\rangle = |\phi\rangle \otimes |\psi\rangle$.

2.1.1 Single Qubit Gates

We now examine the construction and behavior of the single qubit quantum gates: Identity, Pauli-X, Pauli-Y, Pauli-Z, and the Hadamard gate. As we discuss each one, we present the block diagram, show how the operator implementing the transform is created, and comment on the resulting transformation.

The block diagram of the Identity gate is shown in Fig. 1 below:

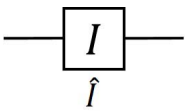

Figure 1 – Block Diagram of the Identity Gate

The Identity gate is basis independent and does not modify the quantum state. The Identity operator, $\hat{I}$, is constructed as shown in Eq. 5:

$$\hat{I} \equiv |0\rangle\langle 0| + |1\rangle\langle 1| = \begin{bmatrix}1 & 0\\0 & 1\end{bmatrix} \quad (5)$$

The Identity operator maintains the quantum state as it maps $|0\rangle \rightarrow |0\rangle$ and $|1\rangle \rightarrow |1\rangle$. The Identity operator is often grouped with the Pauli operators $(\sigma_1, \sigma_2, \sigma_3)$ and when done so is often referred to as σ_0 or σ_I.

The block diagram of the X gate is shown in Fig. 2 below:

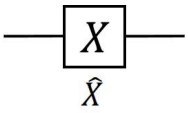

Figure 2 – Block Diagram of the Pauli-X Gate

The Pauli-X gate is the quantum equivalent of the NOT gate for classical computers with respect to the standard basis $|0\rangle$ and $|1\rangle$. The Pauli-X operator, $\hat{X}$, is constructed as shown in Eq. 6:

$$\hat{X} \equiv \sigma_1 = \sigma_X = |1\rangle\langle 0| + |0\rangle\langle 1| = \begin{bmatrix}0 & 1\\1 & 0\end{bmatrix} \quad (6)$$

The Pauli-X operator is often called the "bit-flip" operator as it maps $|0\rangle \rightarrow |1\rangle$ and $|1\rangle \rightarrow |0\rangle$. It generates a rotation around the x axis of the Bloch sphere by π radians.

The block diagram of the Pauli-Y gate is shown in Fig. 3 below:

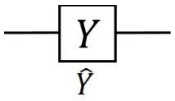

Figure 3 – Block Diagram of the Pauli-Y Gate

The Pauli-Y operator, $\hat{Y}$, is constructed as shown in Eq. 7:

$$\hat{Y} \equiv \sigma_2 = \sigma_Y = i|1\rangle\langle 0| - i|0\rangle\langle 1| = \begin{bmatrix}0 & -i\\i & 0\end{bmatrix} \quad (7)$$

The Pauli-Y operator maps $|0\rangle \rightarrow i|1\rangle$ and $|1\rangle \rightarrow -i|0\rangle$. It generates a rotation around the y axis of the Bloch sphere by π radians.

The block diagram of the Pauli-Z gate is shown in Fig. 4 below:

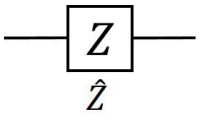

Figure 4 – Block Diagram of the Pauli-Z Gate

The Pauli-Z operator, $\hat{Z}$, is constructed as shown in Eq. 8:

$$\hat{Z} \equiv \sigma_3 = \sigma_Z = |0\rangle\langle 0| - |1\rangle\langle 1| = \begin{bmatrix}1 & 0\\0 & -1\end{bmatrix} \quad (8)$$

The Pauli-Z operator is often called the "phase-flip" operator as it maps $|0\rangle \rightarrow |0\rangle$ and $|1\rangle \rightarrow -|1\rangle$. It generates a rotation around the z axis of the Bloch sphere by π radians.

The Identity gate and Pauli gates, as well as their corresponding operators, are essential elements of the theory of quantum mechanics. As such, it is useful to commit these

gates and operators to memory as they appear frequently in the mathematic representation of quantum mechanics. The Pauli gates and transforms are summarized in Table 1 below.

Table 1 – Pauli Gate Transforms

Quantum Gate	Initial State	Transform	Final State
I	$\|0\rangle$ $\|1\rangle$	$\hat{I} = \sigma_0 = \sigma_I = \begin{bmatrix}1 & 0\\ 0 & 1\end{bmatrix}$	$\|0\rangle = \begin{bmatrix}1\\0\end{bmatrix}$ $\|1\rangle = \begin{bmatrix}0\\1\end{bmatrix}$
X	$\|0\rangle$ $\|1\rangle$	$\hat{X} = \sigma_1 = \sigma_X = \begin{bmatrix}0 & 1\\ 1 & 0\end{bmatrix}$	$\|1\rangle = \begin{bmatrix}0\\1\end{bmatrix}$ $\|0\rangle = \begin{bmatrix}1\\0\end{bmatrix}$
Y	$\|0\rangle$ $\|1\rangle$	$\hat{Y} = \sigma_2 = \sigma_Y = \begin{bmatrix}0 & -i\\ i & 0\end{bmatrix}$	$i\|1\rangle = i\begin{bmatrix}0\\1\end{bmatrix}$ $-i\|0\rangle = -i\begin{bmatrix}1\\0\end{bmatrix}$
Z	$\|0\rangle$ $\|1\rangle$	$\hat{Z} = \sigma_3 = \sigma_Z = \begin{bmatrix}1 & 0\\ 0 & -1\end{bmatrix}$	$\|0\rangle = \begin{bmatrix}1\\0\end{bmatrix}$ $-\|1\rangle = \begin{bmatrix}0\\-1\end{bmatrix}$

Another important single qubit gate is the Hadamard gate which is used to generate superposition states. The block diagram of the Hadamard gate is shown in Fig. 5 below:

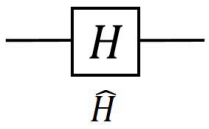

Figure 5 – Block Diagram of the Hadamard Gate

The Hadamard gate generates the superposition states $|+\rangle$ and $|-\rangle$ from the basis states $|0\rangle$ and $|1\rangle$. The Hadamard operator, $\hat{H}$, is constructed as shown in Eq. 9:

$$\hat{H} \equiv |+\rangle\langle 0| + |-\rangle\langle 1| = \frac{1}{\sqrt{2}}\begin{bmatrix}1 & 1\\ 1 & -1\end{bmatrix} \tag{9}$$

The Hadamard operator is the "superposition" operator as it maps $|0\rangle \rightarrow |+\rangle$ and $|1\rangle \rightarrow |-\rangle$. The Hadamard operator generates a rotation of π about the axis $(\hat{x}+\hat{z})/\sqrt{2}$ of the Bloch sphere. The Hadamard transform summary is shown in Table 2.

Table 2 - Hadamard Gate Transform

Initial State	Transform	Final State
$\|0\rangle = \begin{bmatrix}1\\0\end{bmatrix}$	$\frac{1}{\sqrt{2}}\begin{bmatrix}1 & 1\\ 1 & -1\end{bmatrix}$	$\|+\rangle = \frac{(\|0\rangle + \|1\rangle)}{\sqrt{2}}$
$\|1\rangle = \begin{bmatrix}0\\1\end{bmatrix}$	$\frac{1}{\sqrt{2}}\begin{bmatrix}1 & 1\\ 1 & -1\end{bmatrix}$	$\|-\rangle = \frac{(\|0\rangle - \|1\rangle)}{\sqrt{2}}$
$\alpha\|0\rangle + \beta\|1\rangle$	$\frac{1}{\sqrt{2}}\begin{bmatrix}1 & 1\\ 1 & -1\end{bmatrix}$	$\alpha\frac{(\|0\rangle + \|1\rangle)}{\sqrt{2}} + \beta\frac{(\|0\rangle - \|1\rangle)}{\sqrt{2}}$

2.1.2 Two Qubit Gates

We now present the controlled-NOT ($CNOT$) or controlled-X quantum gate. The $CNOT$ gate accepts two qubits as input $|Control\rangle$ and $|Target_{IN}\rangle$, and produces two qubits as output $|Control\rangle$ and $|Target_{OUT}\rangle$ as shown in Fig. 6 below:

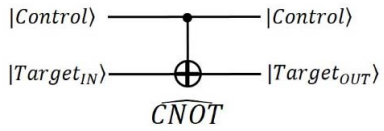

Figure 6 – Block Diagram of the CNOT Gate

In the $CNOT$ gate, the upper $|Control\rangle$ qubit remains unchanged. In contrast, the lower $|Target_{IN}\rangle$ is transformed to $|Target_{OUT}\rangle$ based upon the value of the $|Control\rangle$ qubit. If the $|Control\rangle$ qubit is $|0\rangle$, the $|Target_{OUT}\rangle$ qubit is equal to the $|Target_{IN}\rangle$ qubit. If the $|Control\rangle$ qubit is $|1\rangle$, $|Target_{OUT}\rangle = \hat{X}|Target_{OUT}\rangle$. The gate CNOT is essential in generating maximally entangled Bell state pairs. Table 3 summarizes the CNOT transform.

Table 3 - CNOT Gate Transform

Initial State	Transform	Final State
$\|00\rangle$	$\widehat{CNOT} \equiv \begin{bmatrix}1 & 0 & 0 & 0\\ 0 & 1 & 0 & 0\\ 0 & 0 & 0 & 1\\ 0 & 0 & 1 & 0\end{bmatrix}$	$\|00\rangle$
$\|01\rangle$	$\widehat{CNOT} \equiv \begin{bmatrix}1 & 0 & 0 & 0\\ 0 & 1 & 0 & 0\\ 0 & 0 & 0 & 1\\ 0 & 0 & 1 & 0\end{bmatrix}$	$\|01\rangle$
$\|10\rangle$	$\widehat{CNOT} \equiv \begin{bmatrix}1 & 0 & 0 & 0\\ 0 & 1 & 0 & 0\\ 0 & 0 & 0 & 1\\ 0 & 0 & 1 & 0\end{bmatrix}$	$\|11\rangle$
$\|11\rangle$	$\widehat{CNOT} \equiv \begin{bmatrix}1 & 0 & 0 & 0\\ 0 & 1 & 0 & 0\\ 0 & 0 & 0 & 1\\ 0 & 0 & 1 & 0\end{bmatrix}$	$\|10\rangle$

3 Bell State Generation (BSG) Block

The Bell State Generation (BSG) block is used to generate one of the four maximally entangled *Bell states*. When two qubits are maximally entangled, the probabilities of each qubit are no longer independent. That is, both qubits will be found to be perfectly correlated when measured. This result holds even when the two Bell pair qubits are separated by some arbitrary large distance. By definition, Bell states cannot be written as a tensor product of two *ket* vectors. The Bell State Generation (BSG) block shown in Fig. 7 below and consists of a Hadamard gate and a CNOT gate.

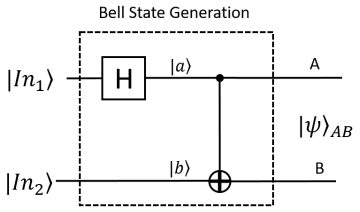

Figure 7 – Bell State Generation (BSG) Block

The BSG block accepts two input qubits $|In_1\rangle$ and $|In_2\rangle$ and generates a joint output state $|\psi_{AB}\rangle$ that is one of the four maximally entangled Bell states: Phi Plus $|\Phi^+\rangle$, Psi Plus $|\Psi^+\rangle$, Phi Minus $|\Phi^-\rangle$, Psi Minus $|\Psi^-\rangle$ as shown in Table 4 below.

Table 4 – Bell State Generator (BSG) Input and Outputs

Qubit Inputs $|In_1\rangle$, $|In_2\rangle$	**Joint State Output** $|\psi\rangle_{AB}$
$\|0\rangle, \|0\rangle$	$\|\Phi^+\rangle_{AB} = \frac{1}{\sqrt{2}}(\|00\rangle_{AB} + \|11\rangle_{AB})$
$\|0\rangle, \|1\rangle$	$\|\Psi^+\rangle_{AB} = \frac{1}{\sqrt{2}}(\|01\rangle_{AB} + \|10\rangle_{AB})$
$\|1\rangle, \|0\rangle$	$\|\Phi^-\rangle_{AB} = \frac{1}{\sqrt{2}}(\|00\rangle_{AB} - \|11\rangle_{AB})$
$\|1\rangle, \|1\rangle$	$\|\Psi^-\rangle_{AB} = \frac{1}{\sqrt{2}}(\|01\rangle_{AB} - \|10\rangle_{AB})$

To understand the operation of the BSG block, let us consider generation of the Phi Plus Bell state, $|\psi\rangle_{AB} = |\Phi^+\rangle$. In this case, the qubit inputs are $|In_1\rangle = |0\rangle$ and $|In_2\rangle = |0\rangle$ and the states at $|a\rangle$ and $|b\rangle$ are shown in Eq. 10 and Eq. 11 respectively.

$$|a\rangle = \hat{H}|0\rangle = \frac{1}{\sqrt{2}}\begin{bmatrix}1 & 1\\ 1 & -1\end{bmatrix}\begin{bmatrix}1\\0\end{bmatrix} = \frac{1}{\sqrt{2}}\begin{bmatrix}1\\1\end{bmatrix} \quad (10)$$

$$|b\rangle = |0\rangle = \begin{bmatrix}1\\0\end{bmatrix} \quad (11)$$

Before we can apply the CNOT gate, we must first calculate the joint state of $|a\rangle$ and $|b\rangle$ as shown in Eq. 12:

$$a \otimes b = \frac{1}{\sqrt{2}}\begin{bmatrix}1\\1\end{bmatrix} \otimes \begin{bmatrix}1\\0\end{bmatrix} = \frac{1}{\sqrt{2}}\begin{bmatrix}1\\0\\1\\0\end{bmatrix} \quad (12)$$

Finally, we apply the CNOT operator to obtain the Phi Plus Bell state $|\Phi^+\rangle_{AB}$ as shown in Eq. 13:

$$|\psi\rangle_{AB} = \widehat{CNOT}(a \otimes b) = \begin{bmatrix}1 & 0 & 0 & 0\\ 0 & 1 & 0 & 0\\ 0 & 0 & 0 & 1\\ 0 & 0 & 1 & 0\end{bmatrix}\frac{1}{\sqrt{2}}\begin{bmatrix}1\\0\\1\\0\end{bmatrix} = \frac{1}{\sqrt{2}}\begin{bmatrix}1\\0\\0\\1\end{bmatrix} = \frac{1}{\sqrt{2}}(|00\rangle_{AB} + |11\rangle_{AB}) = |\Phi^+\rangle_{AB} \quad (13)$$

Note that each of the other three maximally entangled Bell states (Psi Plus $|\Psi^+\rangle$, Phi Minus $|\Phi^-\rangle$, Psi Minus $|\Psi^-\rangle$) can be generated by simply changing the inputs to the BSG block as shown in Table 4.

4 Bell State Measurement (BSM) Block

The Bell State Measurement (BSM) block is used to measure a two-qubit joint state in the Bell basis. The Bell State Measurement (BSM) block shown in Fig. 8 below and consists of a CNOT gate, a Hadamard gate, and two measurement blocks. The double lines to the right of the measurement blocks indicate the output is a classical bit. Thus, the quantum state $|a\rangle$ is measured and collapses into classical bit $b_1 \in \{0,1\}$. Similarly, the quantum state $|b\rangle$ is measured and collapses into classical bit $b_2 \in \{0,1\}$.

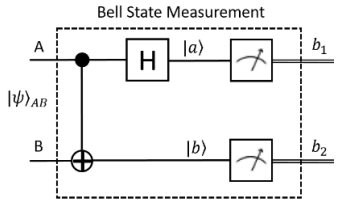

Figure 8 – Bell State Measurement (BSM) Block

The BSM block accepts a joint state $|\psi_{AB}\rangle$ that is one of the four maximally entangled Bell states: Phi Plus $|\Phi^+\rangle$, Psi Plus $|\Psi^+\rangle$, Phi Minus $|\Phi^-\rangle$, Psi Minus $|\Psi^-\rangle$ as shown in Table 4 below.

Table 5 – Bell State Measurement (BSM) Input and Outputs

Joint State Input $|\psi\rangle_{AB}$	**Classical Bit Outputs** b_1 **and** b_2
$\|\Phi^+\rangle_{AB} = \frac{1}{\sqrt{2}}(\|00\rangle_{AB} + \|11\rangle_{AB})$	$b_1 = 0$ $b_2 = 0$
$\|\Psi^+\rangle_{AB} = \frac{1}{\sqrt{2}}(\|01\rangle_{AB} + \|10\rangle_{AB})$	$b_1 = 0$ $b_2 = 1$
$\|\Phi^-\rangle_{AB} = \frac{1}{\sqrt{2}}(\|00\rangle_{AB} - \|11\rangle_{AB})$	$b_1 = 1$ $b_2 = 0$
$\|\Psi^-\rangle_{AB} = \frac{1}{\sqrt{2}}(\|01\rangle_{AB} - \|10\rangle_{AB})$	$b_1 = 1$ $b_2 = 1$

Note that the Bell State Measurement (BSM) block is the reverse of the Bell State Generation (BSG) block.

5 Cascading the BSG and BSM Blocks

There is value in understanding the BSG and BSM as fundamental building blocks to construct more complex quantum circuits. A deeper insight into the quantum circuits is gained by considering the cascade of a Bell State Generation (BSG) block directly connected to a Bell State Measurement (BSM) block as shown in Fig. 9 below.

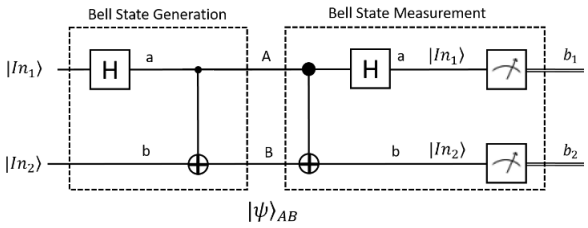

Figure 9 – Cascade of the Bell State Generation (BSG) and Bell State Measurement (BSM) Block

Since quantum gates are reversible and the BSG and BSM are mirrors of each other, the two quantum bits applied to the BSG inputs will appear before the measurement blocks in the BSM and the corresponding classical bits will be deterministic.

6 Superdense Coding Protocol

In this section, we introduce the Superdense Coding protocol which is a stepping stone to understand the Quantum Teleportation protocol. The Superdense Coding protocol uses the BSG and BSM blocks as well as conditional X and Z gates as shown in Fig. 10. In this example, BSG block is used to generate the Phi Plus $|\Phi^+\rangle_{AB}$ Bell state. However, any of the four maximally entangled Bell states can be used with minor circuit modifications by adding classical inverters before the conditional X and Z gates in the circuit.

The goal of the Superdense Coding protocol for *Alice* to send two classical bits of information to *Bob* by changing her half of the EPR pair shared with *Bob*. Superdense Coding protocol was first proposed by Bennett and Wiesner in 1970 [5], but not published until 1992 [6]. It was first experimentally implemented in 1996 by Mattle, Weinfurter, Kwiat and Zeilinger using entangled photon pairs [7]. The Superdense Coding protocol (1992) was a precursor to the Quantum Teleportation protocol (1993) [8]. The Quantum Teleportation protocol is often considered as a flipped version of the Superdense Coding protocol.

Superdense Coding works by *Alice* changing her half of a shared EPR pair using a conditional X and conditional Z block based upon two input classical bits b_2 and b_1 that she wishes to send to *Bob*. By transforming her half of the EPR pair, she can change the joint state seen by *Bob* from Phi Plus $|\Phi^+\rangle_{AB}$ to Psi Plus $|\Psi^+\rangle_{AB}$, Phi Minus $|\Phi^-\rangle_{AB}$, or Psi Minus $|\Psi^-\rangle_{AB}$. As we have seen in the last section, if *Bob* receives any of these states, he will measure a deterministic output from his BSM block. For example, if $b_2 = 0$ and $b_1 = 0$, then the conditional X and conditional Z are simply Identity gates. As a consequence, the joint quantum state seen by *Bob* is unchanged Phi Plus $|\Phi^+\rangle_{AB}$ and the resulting classical bits output are ${b_1}' = 0$ and ${b_2}' = 0$. If *Alice* wishes to send $b_2 = 1$ and $b_1 = 0$, then the conditional X is active and the conditional Z is an Identity gate. The impact of applying an X gate to *Alice's* half of the EPR pair is to change the joint quantum state seen by *Bob* to Psi Plus $|\Psi^+\rangle_{AB}$ and the resulting classical bits output are ${b_1}' = 0$ and ${b_2}' = 1$. If *Alice* wishes to send $b_2 = 0$ and $b_1 = 1$, then the conditional Z is active and the conditional X is an Identity gate. The impact of applying an Z gate to *Alice's* half of the EPR pair is to change the joint quantum state seen by *Bob* to Phi Minus $|\Phi^-\rangle_{AB}$ and the resulting classical bits output are ${b_1}' = 1$ and ${b_2}' = 0$. Finally, if *Alice* wishes to send $b_2 = 1$ and $b_1 = 1$, then the conditional X and conditional Z gates are active. The impact of applying an X gate and a Z gate to *Alice's* half of the EPR pair is to change the joint quantum state seen by *Bob* to Psi Minus $|\Psi^-\rangle_{AB}$ and the resulting classical bits output are ${b_1}' = 1$ and ${b_2}' = 1$.

Table 6 – Superdense Coding Inputs and Outputs

Alice's Transmitted Message b_1 and b_2	**Alice's Applied Unitary Transforms**	**Two Qubit Joint State at Bob**	**Bob's Received Message ${b_1}'$ and ${b_2}'$**
$b_1 = 0$ $b_2 = 0$	$I * I$	$\|\Phi^+\rangle_{AB} = \frac{1}{\sqrt{2}}(\|00\rangle_{AB} + \|11\rangle_{AB})$	${b_1}' = 0$ ${b_2}' = 0$
$b_1 = 0$ $b_2 = 1$	$I * X$	$\|\Psi^+\rangle_{AB} = \frac{1}{\sqrt{2}}(\|01\rangle_{AB} + \|10\rangle_{AB})$	${b_1}' = 0$ ${b_2}' = 1$
$b_1 = 1$ $b_2 = 0$	$Z * I$	$\|\Phi^-\rangle_{AB} = \frac{1}{\sqrt{2}}(\|00\rangle_{AB} - \|11\rangle_{AB})$	${b_1}' = 1$ ${b_2}' = 0$
$b_1 = 1$ $b_2 = 1$	$Z * X$	$\|\Psi^-\rangle_{AB} = \frac{1}{\sqrt{2}}(\|01\rangle_{AB} - \|10\rangle_{AB})$	${b_1}' = 1$ ${b_2}' = 1$

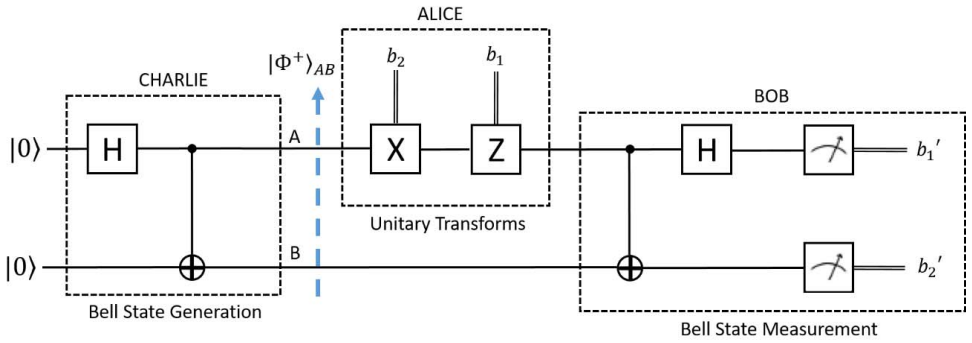

Figure 10 – Superdense Coding Protocol Quantum Gate Diagram

7 Quantum Teleportation Protocol

In this section, we introduce the Quantum Teleportation protocol which is the essential element used in quantum networks [8]. The Quantum Teleportation protocol was first proposed by Bennett, Brassard, Crépeau, Jozsa, Peres, and Wootters in 1993 [8]. It was first experimentally implemented in 1997 by two research groups: one led by Sandu Popescu and the other by Anton Zeilinger [9]. Experimental quantum teleportation has been demonstrated using photons, atoms, electrons, and superconducting circuits over distances up to 1,400 km by Jian-Wei Pan's group using the Micius satellite for space-based quantum teleportation.

The goal of the Quantum Teleportation protocol is to send an unknown quantum state $|\psi\rangle_C$ from one point to another using a shared EPR pair and two classical bits. Fig. 11 shows the quantum gate diagram for Quantum Teleportation. The protocol accepts an unknown quantum state $|\psi\rangle_C$ and uses the BSG block (*Charlie*), the BSM block (*Alice*), and the conditional X and Z gates (*Bob*). In this example, *Charlie* generates the Phi Plus $|\Phi^+\rangle_{AB}$ maximally entangled Bell state. However, just as in the Superdense Coding discussed above, any of the three other maximally entangled Bell states can be used with appropriate adjustments in the circuit.

In this circuit, *Charlie* shares half of the EPR pair with *Alice* and the other half with *Bob*. *Alice* conducts a Bell state measurement of the unknown quantum state and her half of the EPR pair which collapses the state and instantaneously communicates information to *Bob's* half of the EPR pair. *Alice* communicates the outcomes of the BSM measurement, b_2 and b_1, to *Bob* through a classical channel. *Bob* then applies the appropriate unitary transforms to his half of the EPR pair to recover the unknown quantum state. *Bob* applies a Pauli-Z operator when $b_1 = 1$ and a Pauli-X operator when $b_2 = 1$. The result of the protocol is that *Bob* has transformed his half of the EPR pair into $|\psi\rangle_C{}'$ based upon the results of *Alice's* Bell state measurement. Note that in our discussion we are presenting the ideal case when there are no errors or noise, so $|\psi\rangle_C = |\psi\rangle_C{}'$.

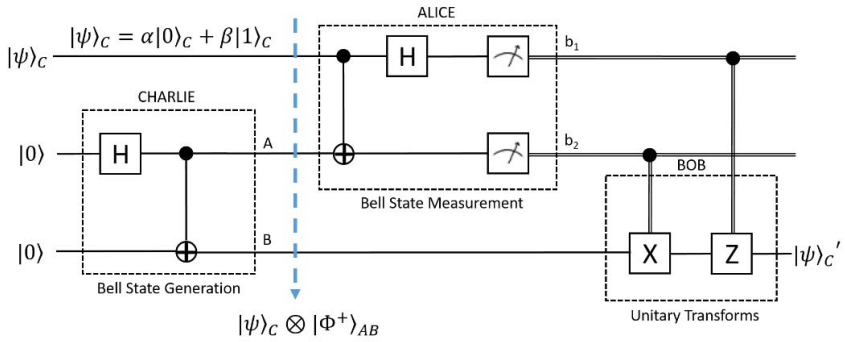

Figure 11 – Quantum Teleportation Protocol Quantum Gate Diagram

The key insight into understanding how the Quantum Teleportation protocol works is to understand that conducting a Bell state measurement forces the qubits that are input to the BSM block to collapse. Specifically, if the two qubits applied to the BSM block are part of a larger joint state, the measurement results of the BSM reveal which elements of the larger joint state still exist. In our view, this is the "secret sauce" in understanding the Quantum Teleportation protocol works. Once you grasp this concept, analysis of the rest of the protocol is simple algebraic manipulations. For this reason, it is useful to first rewrite qubits pairs in terms of the sums and differences of the four maximally entangled Bell states. When a Bell measurement occurs, it collapses the joint state in the given Bell basis. The results of the Bell state measurement reveal valuable information when the measured qubits are part of a larger joint state. Rewriting the terms in a joint state using this substitution is very similar to rewriting a state using a change of basis. Table 7 summarizes how you can rewrite a two qubit joint state as the sum or difference of two maximally entangled Bell states. It is not difficult to prove the equivalent representations shown in Table 7 and we encourage the reader to do so.

Table 7 – Equivalent Representation of Two Qubit Joint States Input to a BSM using Sums and Differences of Bell States in The Bell Basis

Two-Qubit Joint State Input to a BSM	Equivalent Representation using Sums and Differences of Bell States
$\|0\rangle \otimes \|0\rangle = \|00\rangle$	$\frac{1}{\sqrt{2}}(\|\Phi^+\rangle + \|\Phi^-\rangle)$
$\|0\rangle \otimes \|1\rangle = \|01\rangle$	$\frac{1}{\sqrt{2}}(\|\Psi^+\rangle + \|\Psi^-\rangle)$
$\|1\rangle \otimes \|0\rangle = \|10\rangle$	$\frac{1}{\sqrt{2}}(\|\Psi^+\rangle - \|\Psi^-\rangle)$
$\|1\rangle \otimes \|1\rangle = \|11\rangle$	$\frac{1}{\sqrt{2}}(\|\Phi^+\rangle - \|\Phi^-\rangle)$

Now that we have the required tools to analyze the Quantum Teleportation circuit, we first must calculate the three qubit joint state highlighted in Fig. 11. This calculation is shown in Eq. 13 below and consists of taking the tensor product of the unknown quantum state to be teleported, $|\psi\rangle_C$, and the BSG output, $|\Phi^+\rangle_{AB}$ as shown in Eq. 14 below:

$$|\psi\rangle_C \otimes |\Phi^+\rangle_{AB} = (\alpha|0\rangle_C + \beta|1\rangle_C) \otimes \frac{1}{\sqrt{2}}(|00\rangle_{AB} + |11\rangle_{AB}) =$$

$$\frac{1}{\sqrt{2}}(\alpha|000\rangle_{CAB} + \alpha|011\rangle_{CAB} + \beta|100\rangle_{CAB} + \beta|111\rangle_{CAB}) =$$

$$\frac{1}{\sqrt{2}}(\alpha|00\rangle_{CA} \otimes |0\rangle_B + \alpha|01\rangle_{CA} \otimes |1\rangle_B + \beta|10\rangle_{CA} \otimes |0\rangle_B + \beta|11\rangle_{CA} \otimes |1\rangle_B) =$$

$$\tfrac{1}{\sqrt{2}}(\alpha|00\rangle_{CA} \otimes |0\rangle_B) + \tfrac{1}{\sqrt{2}}(\alpha|01\rangle_{CA} \otimes |1\rangle_B) + \tfrac{1}{\sqrt{2}}(\beta|10\rangle_{CA} \otimes |0\rangle_B) + \tfrac{1}{\sqrt{2}}(\beta|11\rangle_{CA} \otimes |1\rangle_B) \quad (14)$$

After writing the tensor product of the three qubits, we grouped the unknown qubit state to be teleported, $|\psi\rangle_C$, and the *A* half qubit of the BSG output $|\Phi^+\rangle_{AB}$ together and refer to this with subscript *CA*. We did this as we recognize the two qubit joint state that is input into the BSM is part of a larger joint state. The next step is to apply the equivalent substitutions from Table 7 for each of the possible two qubit pairs as shown in Eqs. 15, 16, 17, and 18:

$$\tfrac{1}{\sqrt{2}}(\alpha|00\rangle_{CA} \otimes |0\rangle_B) = \alpha\tfrac{1}{2}(|\Phi^+\rangle_{CA} + |\Phi^-\rangle_{CA}) \otimes |0\rangle_B \quad (15)$$

$$\tfrac{1}{\sqrt{2}}(\alpha|01\rangle_{CA} \otimes |1\rangle_B) = \alpha\tfrac{1}{2}(|\Psi^+\rangle_{CA} + |\Psi^-\rangle_{CA}) \otimes |1\rangle_B \quad (16)$$

$$\tfrac{1}{\sqrt{2}}(\beta|10\rangle_{CA} \otimes |0\rangle_B) = \beta\tfrac{1}{2}(|\Psi^+\rangle_{CA} - |\Psi^-\rangle_{CA}) \otimes |0\rangle_B \quad (17)$$

$$\tfrac{1}{\sqrt{2}}(\beta|11\rangle_{CA} \otimes |1\rangle_B) = \beta\tfrac{1}{2}(|\Phi^+\rangle_{CA} - |\Phi^-\rangle_{CA}) \otimes |1\rangle_B \quad (18)$$

Next, we rewrite Eq. 14 using the substitutions shown in Eqs. 15, 16, 17, and 18 as the result is shown in Eq. 19:

$$|\psi\rangle_C \otimes |\Phi^+\rangle_{AB} = (\alpha|0\rangle_C + \beta|1\rangle_C) \otimes \frac{1}{\sqrt{2}}(|00\rangle_{AB} + |11\rangle_{AB}) =$$

$$\frac{1}{\sqrt{2}}(\alpha|00\rangle_{CA} \otimes |0\rangle_B) + \frac{1}{\sqrt{2}}(\alpha|01\rangle_{CA} \otimes |1\rangle_B) + \frac{1}{\sqrt{2}}(\beta|10\rangle_{CA} \otimes |0\rangle_B) + \frac{1}{\sqrt{2}}(\beta|11\rangle_{CA} \otimes |1\rangle_B) =$$

$$\left(\alpha\frac{1}{2}(|\Phi^+\rangle_{CA} + |\Phi^-\rangle_{CA}) \otimes |0\rangle_B\right) + \left(\alpha\frac{1}{2}(|\Psi^+\rangle_{CA} + |\Psi^-\rangle_{CA}) \otimes |1\rangle_B\right) +$$

$$\left(\beta\tfrac{1}{2}(|\Psi^+\rangle_{CA} - |\Psi^-\rangle_{CA}) \otimes |0\rangle_B\right) + \left(\beta\tfrac{1}{2}(|\Phi^+\rangle_{CA} - |\Phi^-\rangle_{CA}) \otimes |1\rangle_B\right) \quad (19)$$

Note that Eq. 19 is now written in terms of the Bell states in the Bell basis, so the results of a Bell state measurement will provide valuable information about the *B* qubit in the other half of the EPR pair after measurement. Next, we expand Eq. 19 and collect the Bell state terms to reveal which portions of the larger three qubit joint state remain after measurement as shown in Eq. 20:

$$|\psi\rangle_C \otimes |\Phi^+\rangle_{AB} =$$

$$= \alpha\frac{1}{2}|\Phi^+\rangle_{CA} \otimes |0\rangle_B + \alpha\frac{1}{2}|\Phi^-\rangle_{CA} \otimes |0\rangle_B + \alpha\frac{1}{2}|\Psi^+\rangle_{CA} \otimes |1\rangle_B + \alpha\frac{1}{2}|\Psi^-\rangle_{CA} \otimes |1\rangle_B +$$

$$\beta\frac{1}{2}|\Psi^+\rangle_{CA} \otimes |0\rangle_B - \beta\frac{1}{2}|\Psi^-\rangle_{CA} \otimes |0\rangle_B + \beta\frac{1}{2}|\Phi^+\rangle_{CA} \otimes |1\rangle_B - \beta\frac{1}{2}|\Phi^-\rangle_{CA} \otimes |1\rangle_B =$$

$$\tfrac{1}{2}[|\Phi^+\rangle_{CA} \otimes (\alpha|0\rangle_B + \beta|1\rangle_B) + |\Phi^-\rangle_{CA} \otimes (\alpha|0\rangle_B - \beta|1\rangle_B) + |\Psi^+\rangle_{CA} \otimes (\alpha|1\rangle_B + \beta|0\rangle_B) + |\Psi^-\rangle_{CA} \otimes (\alpha|1\rangle_B - \beta|0\rangle_B)] \quad (20)$$

It is important to note that all three qubits shown in Eq. 20 are still in the same total state since no measurement has yet been performed. Instead, we have simply performed a change of basis in *Alice's* part of the system. The actual teleportation occurs when *Alice* conducts her Bell state measurement and measures qubits in the Bell basis $(|\Phi^+\rangle_{CA}, |\Phi^-\rangle_{CA}, |\Psi^+\rangle_{CA}, |\Psi^-\rangle_{CA})$.

Alice's local measurement of the joint state collapses two of the qubits into one of the four states with equal probability (25%). After the Bell state measurement is completed, *Alice* sends the two classical bits resulting from the Bell state measurement to *Bob* over a classical channel informing him of the result. *Bob's* half of the EPR pair, $|\psi\rangle_B$, instantaneously becomes one of the four corresponding superposition states shown in Table 8. The Bell state measurement causes the joint state to collapse leaving $|\psi\rangle_B$ in a known state.

Now, *Bob* simply has to perform a unitary transform to recover the original state based upon the two classical bits b_2 and b_1 resulting from the Bell state measurement that *Alice* sends him over a classical channel. Bob applies the transforms as shown in Table 9 to recover the state $|\boldsymbol{\psi}\rangle_{\boldsymbol{C}}{}'$. Note that the operators $\hat{I}$, $\hat{X}$, and $\hat{Z}$ are listed in the mathematical (not physical) order they are applied.

Table 8 – Results of Alice's Bell State Measurement and the Corresponding State of Bob's Half of the EPR Pair

Alice's Bell State Measurement Result	State of Bob's Half of the EPR Pair $\|\psi\rangle_B$
$\|\Phi^+\rangle_{CA}$	$(\alpha\|0\rangle_B + \beta\|1\rangle_B)$
$\|\Phi^-\rangle_{CA}$	$(\alpha\|0\rangle_B - \beta\|1\rangle_B)$
$\|\Psi^+\rangle_{CA}$	$(\alpha\|1\rangle_B + \beta\|0\rangle_B)$
$\|\Psi^-\rangle_{CA}$	$(\alpha\|1\rangle_B - \beta\|0\rangle_B)$

Table 9 – Alice's Bell State Measurement Results and the Corresponding Transformations Required for Bob to Recover the Teleported State $|\psi\rangle_C{}'$

Alice's Bell State Measurement Result	Bob's Transformation of $\|\psi\rangle_B$ to Recover the Teleported State $\|\psi\rangle_C{}'$
$\|\Phi^+\rangle_{CA}$	$\hat{I} * \hat{I}\ (\alpha\|0\rangle + \beta\|1\rangle) = (\alpha\|0\rangle_B + \beta\|1\rangle_B)$
$\|\Phi^-\rangle_{CA}$	$\hat{Z} * \hat{I}\ (\alpha\|0\rangle_B - \beta\|1\rangle_B) = (\alpha\|0\rangle_B + \beta\|1\rangle_B)$
$\|\Psi^+\rangle_{CA}$	$\hat{I} * \hat{X}\ (\alpha\|1\rangle_B + \beta\|0\rangle_B) = (\alpha\|0\rangle_B + \beta\|1\rangle_B)$
$\|\Psi^-\rangle_{CA}$	$\hat{Z} * \hat{X}\ (\alpha\|1\rangle_B - \beta\|0\rangle_B) = (\alpha\|0\rangle_B + \beta\|1\rangle_B)$

8 Conclusions and Future Work

In this paper, we presented a demonstration of how decomposing a complex system into a series of smaller abstract functional blocks can be very helpful in developing comprehensive system understanding. Specifically, we identified and enumerated the basic quantum circuit blocks found in the ideal Quantum Teleportation protocol quantum circuit. We examined the mathematical models used to represent the behavior of each of the quantum circuit blocks and provided some general guidelines on how the blocks behave. We accomplished this by understanding what happens when the quantum basis states are operated upon by the corresponding mathematical operators. We found it is very useful to summarize and understand how each operator acts on the zero state, $|0\rangle$, and the one state, $|1\rangle$ so that when you examine an new quantum circuit, you will have developed some intuition as to how the quantum circuit operates without the need to immediately calculate the model outputs.

We then closely examined how the Bell State Generation (BSG) and Bell State Measurement (BSM) blocks operate to create and measure maximally entangled Bell states. We showed how developing a basic understanding of these blocks simplifies the analysis of quantum circuit that consists of a cascade of a BSG block with a BSM block. Next, built on this finding by introducing the Superdense Coding protocol and quantum circuit. We saw how adding the single qubit blocks $\hat{X}$ and $\hat{Z}$ enabled *Alice* to change her half the EPR pair to transform the joint state seen by *Bob* to from Phi Plus $|\Phi^+\rangle_{AB}$ to Psi Plus $|\Psi^+\rangle_{AB}$, Phi Minus $|\Phi^-\rangle_{AB}$, or Psi Minus $|\Psi^-\rangle_{AB}$. As a consequence, when *Bob* conducts his Bell state measurement, he will obtain the classical bits that *Alice* desired to send him using the quantum channel. At this point, we showed how quantum states can be manipulated to attain the goal of *Alice* sending two classical bits of information to *Bob* by changing her half of the EPR pair shared with *Bob*.

Finally, we examined the Quantum Teleportation protocol and quantum circuit. We found that all of the functional blocks found in the Superdense Coding circuit were also present in Quantum Teleportation circuit, but with the addition of an unknown quantum state. We then presented the mathematical calculations required to understand how a three qubit joint state can be manipulated by a Bell state measurement. We showed the key insight into understanding how the Quantum Teleportation protocol works is to understand that conducting a Bell state measurement forces the qubits that are input to the BSM block to collapse. Specifically, if the two qubits applied to the BSM block are part of a larger joint state, the measurement results of the BSM reveal which elements of the larger joint state still exist. We then showed how Bob can recover the unknown quantum state by manipulating the joint quantum state using the operators $\hat{I}$, $\hat{X}$, and $\hat{Z}$.

Our hope is that this paper enables the reader to more easily gain a deeper insight and to develop a better understanding of how to analyze quantum circuit implementations of quantum protocols. While this information is introductory in nature, it can provide value to those who are new to modeling, simulating, and analyzing ideal quantum circuits.

Disclaimer

The views expressed in this paper are those of the authors and do not reflect the official policy or position of the U.S. Air Force, the Department of Defense, or the U.S. Government.

9 References

[1] Gisin, N., Thew, R. Quantum communication. Nature Photon 1, 165–171 (2007). https://doi.org/10.1038/nphoton.2007.22

[2] R. Van Meter, Quantum Networking, vol. 9781848215375. 2014.

[3] Scarani, V., Iblisdir, S., Gisin, N., and Acín, A. Quantum cloning. Rev. Mod. Phys. 77, 1225 (2005). https://arxiv.org/abs/quant-ph/0511088

[4] J. Watrous, "The Theory of Quantum Information," Theory Quantum Inf., (2018).

[5] Wiesner, S., "Conjugate Coding". ACM SIGACT News. Vol. 15, No. 1, pp. 78–88, Winter-Spring 1983.

[6] Bennett, C. and Wiesner, S., "Communication via one- and two-particle operators on Einstein-Podolsky-Rosen states". Phys. Rev. Lett. 69, (20): 2881–2884 (1992).

[7] Mattle, K., Weinfurter, H., Kwiat, P.G., and Zeilinger, A., "Dense Coding in Experimental Quantum Communication". Phys. Rev. Lett. 76, 4656 (1996).

[8] Bennett, C.H., Brassard, G., Crépeau, C., Jozsa, R., Peres, A., and Wootters, W. K., "Teleporting an Unknown Quantum State via Dual Classical and Einstein–Podolsky–Rosen Channels." Phys. Rev. Lett. 70 (13): 1895–1899 (1993).

[9] Yurke, B. & Stoler, D., "Bell's-inequality experiments using independent-particle sources." Phys. Rev. A 46, 2229–2234 (1992).